Longitudinal Effects of Single Hindlimb Radiation Therapy on Bone Strength and Morphology at Local and Contralateral Sites

Megan E Oest, PhD[*,1], **Connor G Policastro, BS**[1], **Kenneth A Mann, PhD**[1], **Nicholas D Zimmerman, MS**[1], and **Timothy A Damron, MD**[1]

[1]SUNY Upstate Medical University Department of Orthopedics, Syracuse NY

Abstract

Radiation therapy (RTx) is associated with increased risk for late-onset fragility fractures in bone tissue underlying the radiation field. Bone tissue outside the RTx field is often selected as a "normal" comparator tissue in clinical assessment of fragility fracture risk, but the robustness of this comparison is limited by an incomplete understanding of the systemic effects of local radiotherapy. In this study, a mouse model of limited field irradiation was used to quantify longitudinal changes in local (irradiated) and systemic (non-irradiated) femurs with respect to bone density, morphology, and strength. BALB/cJ mice aged 12 weeks underwent unilateral hindlimb irradiation (4x5 Gy) or a sham procedure. Femurs were collected at end points of 4 days prior to treatment, and 0, 1, 2, 4, 8, 12, and 26 weeks post-treatment. Irradiated (RTx), Contralateral (non-RTx), and Sham (non-RTx) femurs were imaged by micro-computed tomography and mechanically tested in three-point bending. In both the RTx and Contralateral non-RTx groups, the longer-term (12-26 week) outcomes included trabecular resorption, loss of diaphyseal cortical bone, and decreased bending strength. Contralateral femurs generally followed an intermediate response compared to RTx femurs. Change also varied by anatomic compartment; post-RTx loss of trabecular bone was more profound in the metaphyseal than the epiphyseal compartment, and cortical bone thickness decreased at the mid-diaphysis but increased at the metaphysis. These data demonstrate that changes in bone quantity, density, and architecture occur both locally and systemically following limited field irradiation and vary by anatomic compartment. Furthermore, the severity and persistence of systemic bone damage following limited field irradiation suggest selection of control tissues for assessment of fracture risk or changes in bone density following radiotherapy may be challenging.

Keywords

biomechanics; fracture risk assessment; preclinical studies; bone µCT; radiation-induced bone disease

INTRODUCTION

Radiation therapy (RTx) is a clinically effective component of oncologic care. However, late-onset bone fragility fractures are a complication in 4-33% of survivors.[1-4] Post-radiotherapy fragility fractures—which occur months to years after treatment in otherwise healthy bone that was included in the radiation field—are difficult to predict in part due to an incomplete understanding of the pathophysiology of irradiated bone.

Following radiotherapy, local bone tissue is characterized by trabecular resorption, decreased cellularity, and marrow adiposity.[3,5-7] By contrast, although low bone mineral density (BMD) has been strongly associated with bone fragility in osteoporosis, clinical studies following cancer survivors treated with radiotherapy have not demonstrated a consistent connection between irradiation and decreased bone mass or density within the irradiated field in human studies.[7,8] This lack of mass-strength correlation contributes to the difficulty in accurately predicting post-radiotherapy bone fractures in clinical settings.

The occurrence of post-radiotherapy bone fragility fractures in the absence of osteopenia suggests that reduction in bone quality (material strength) or bone tissue distribution (geometry) may also contribute to post-radiotherapy fracture risk. Animal models have been used extensively to characterize the effects of limited field or focal irradiation on bone pathophysiology. A consistent pattern of increased osteoclastic resorption[9-11] followed by loss of trabecular bone has emerged.[12-14] Bone density is not consistently decreased in irradiated animals, although a consistent pattern of radiation-induced alterations to the tissue matrix has emerged, including increased trivalent:divalent collagen crosslink ratios, formation of pathologic glycation end products, and overly-aligned mineral and collagen phases.[12,15-18] Biomechanical studies have indicated that changes in bone morphology and mineral content alone do not fully explain post-radiotherapy bone fragility, suggesting a role for material embrittlement.[19] Several aspects of radiation damage to bone remain uncharacterized, including: a direct comparison of changes in structural, material, and geometric properties; the temporal progression of bone damage; the extent to which systemic or abscopal effects (responses in tissues distant to the treatment field) occur; and how bone remodeling differs across anatomic compartments. Wright et al. demonstrated decreased bone volume fraction and trabecular thickness in contralateral non-irradiated tibias at a single time point, one week following single hindlimb irradiation of 2 Gy.[13] Similarly, Zou et al. report decreased tissue mineral density in both irradiated and contralateral non-irradiated tibias of rats twelve weeks after a single 20 Gy fraction of radiation.[20] Bending strength was decreased only in the irradiated femur at 12 weeks, and longitudinal responses were not documented. These data indicate that changes in bone quantity, density, and mechanics are temporally complex, potentially variable by anatomic site, and entangled with changes in morphology and tissue quality.

The goal of this study was to quantify the longitudinal effects of limited field irradiation on the morphology and strength of irradiated femurs, contralateral (non-irradiated) femurs, and sham (non-irradiated) control femurs. Using a mouse model of fractionated unilateral hindlimb irradiation, we evaluated changes in trabecular and cortical bone architecture and density at time points ranging from zero to twenty-six weeks post-irradiation. Whole bone

and material strength of irradiated, non-irradiated contralateral, and sham-treated femurs were determined using three-point bending tests at each end point. This mouse model of limited field, fractionated radiotherapy is well established and replicates many aspects of the established human pathologic responses to irradiation including osteocyte death, trabecular bone resorption, marrow adiposity, and increased bone fragility.[5,6,13,19,21]

We *hypothesize* that RTx will reduce bone quantity (size, volume fraction), tissue density in multiple compartments of the femur, and reduce femur and cortical bone strength compared to control (non-irradiated sham) femurs. We further hypothesize that the contralateral (non-irradiated) limb of the irradiated mouse will also have diminished morphology and mechanics parameters. Because there will likely be multiple factors that contribute to overall femur strength, we hypothesize that femur bending strength and post-yield displacement will depend on bone cross-sectional size, diaphyseal tissue mineral density, and the irradiation status of the bone.

METHODS

Fractionated Hindlimb Irradiation Model

All experiments were approved in advance by the Institutional Animal Care and Use Committee, in accordance with the guidelines of the US Public Health Service (Assurance #A3514-01). Female BALB/cJ mice were purchased from Jackson Labs (Bar Harbor, ME) at six weeks of age, and randomly assigned to treatment groups (n=160 mice, with n = 10/ group/time point, except for n = 12 at weeks 12 and 26 for the RTx/Contra and week 26 for Sham mice). Throughout the study, animals were maintained in community housing (n ≤ 5 mice per cage) in an AAALAC-accredited facility and supplied with water and pellet chow (Formulab Diet 5008, LabDiet, St. Louis, MO) *ad libitum*. Investigators were not blinded during animal handling or body weight measurements.

At twelve weeks of age, mice were anesthetized using ketamine/xylazine (100/10 mg/kg IP, #501090/51004, MWI Veterinary Supply, Boise ID), and placed under a 4 mm thick lead shield with the right limb extended beyond the shielding to allow for limited field radiation (Figure 1A). The mice were subjected to unilateral hindlimb irradiation using four consecutive daily doses of 5 Gy[10,22] from a collimated X-ray source (225kV beam at 17mA, Faxitron MultiRad 225, Faxitron Bioptics, Tucson, AZ). The contralateral hindlimb served as a non-irradiated control. Dosimetry for the lead shielding revealed a dose of less than 0.11 Gy penetrated the shielding during each 5 Gy radiation exposure. A second group of mice underwent a mock irradiation (*Sham*) procedure in which they were subjected to the same treatment protocol (handling, anesthesia, recovery) excluding actual irradiation. There were four animal deaths that occurred in the RTx group during the fractionated irradiation treatment period as a result of anesthesia complications. Body mass did not significantly differ between treatment groups at any time point (Figure 1B).

This mouse hindlimb irradiation model mimics several key aspects of clinical radiotherapy, including use of X-rays as the ionizing radiation source, dose fractionation, and treatment of a limited field. The biologically equivalent dose for this treatment protocol was calculated to be 55.7 Gy using the linear quadratic method and assuming an α/β of 2.8 for late-responding

normal tissues.[15,23,24] This is in the range of doses used to treat breast cancer metastases to bone, but below that used to treat chondrosarcoma.[25,26] Unilateral hindlimb irradiation exposes a larger percentage of the mouse's body to irradiation than occurs in most clinical radiotherapy. This hindlimb exposure, however, enables direct biomechanical testing of the bone in multiple loading modalities, something to which focal irradiation of mouse bone is not conducive.

At one time point prior to the first day of irradiation (-0.6 weeks) and at 0, 1, 2, 4, 8, 12, and 26 weeks after the last radiation dose or sham procedure, the mice were euthanized using CO_2 asphyxiation. The femurs were disarticulated, stripped of soft tissues, wrapped in gauze soaked with saline, and stored at -80°C.

Bone Morphology Measures

Femurs were imaged using micro-computed tomography (μCT 40, Scanco, Brüttisellen, Switzerland) at a voxel resolution of 12 μm over the length of the bone. A lower global threshold of 654 mg HA/cm^3 was used to segment bone. Following image reconstruction, four regions of interest (ROI) were evaluated (Figure 1C) using the Scanco software (3D measures) or NIH ImageJ (2D measures). These four ROIs were chosen to represent the main compartments of the femur exposed to the radiation field including the diaphysis, cortical and trabecular metaphysis and epiphyseal metaphysis. The proximal femur was not included in the analysis, because it was not directly in the radiation field. The μCT scans were contoured and evaluated under blinded conditions by a single laboratory technician (NDZ). Cortical area (Ct.Ar), mean cortical thickness (Ct.Th), and total bone area (Tt.Ar, endosteal + cortical area) were calculated for diaphyseal cortical bone at 50% of the femur length. The Ct.Ar and Ct.Th for the metaphyseal cortical bone was measured in a 0.12 mm thick section located 0.05 mm proximal from the superior aspect of the distal femur growth plate. Bone volume fraction (BV/TV), trabecular number (Tb.N), trabecular thickness (Tb.Th), and connectivity density (Conn.D) was determined for a volume of metaphyseal trabecular bone located 0.05 mm proximal to the growth plate with an axial length of 3% of femur length. The same trabecular morphology measures were made for the epiphyseal trabecular bone located immediately proximal to the intercondylar groove and distal to the growth plate (2.8% of femur length). Tissue mineral density (TMD) was determined for the diaphyseal (cortical), metaphyseal (trabecular), and epiphyseal (trabecular) regions. It should be noted that trabecular TMD measures generally require trabeculae that are at least 5 voxels thick (60 μm) in order to allow sufficient volume for accurate TMD determination,[27] While the majority of the epiphyseal trabecular bone meets this criterion, the metaphyseal bone is often only ~4 voxels thick (40-50 μm) making these TMD values less reliable. They are reported here with the understanding that relative comparisons between the treatment groups may be of value, but the absolute measure may not be accurate.

Mechanical Testing

Three-point bend tests were used to determine whole-bone bending mechanics of the mid-diaphysis of the femur and to calculate material (tensile flexural) properties of the cortical bone. Femurs were placed in a three-point bend fixture with a span of 8 mm and stainless steel loading pins with a diameter of 0.8 mm. Femurs were oriented such that the anterior

surface was under tension, and then loaded in displacement control (1 mm/min) until failure using a mechanical test frame (Qtest, MTS corporation, Eden Prarie, MN). Tests were performed in laboratory air at room temperature; hydration was maintained using saline solution prior to testing.

Five measures were used to describe the mechanical response of the femur in three-point bend (Figure 1D). *Bending strength* was determined at the peak applied load, *bending stiffness* was calculated using the initial slope of the moment-displacement curve, *post yield displacement* was calculated as the distance from the yield point to complete failure of the bone, and *energy to break* was calculated as the area under the moment-displacement curve. The yield offset (*d*) was calculated using

$$d = \varepsilon \frac{S^2}{12c} \quad \text{[Eqn 1]}$$

where *ε* is the 0.2% strain offset, *S* is the span, and *c* is the distance from the neutral (centroidal) axis and most anterior fiber (i.e., the most anterior aspect of cortical tissue) in the cross section. The *normalized bending strength*, calculated as the femur bending strength divided by mouse weight, was used to provide a measure of resistance to fracture, as femur loading would be proportional to body weight.

Three measures were used to describe the stress-strain response of the anterior surface of the cortical bone during loading. The flexural stress (*σ*) on the anterior surface of the bone was calculated using nonsymmetric beam equations:[28]

$$\sigma = \frac{M \cos\phi y'}{I'_z} + \frac{M \sin\phi z'}{I'_y} \quad \text{[Eqn 2]}$$

with *M* as the applied moment, area moment of inertia properties (I'_z, I'_y) about the 'primed' coordinate system oriented at an angle *ϕ* with respect to the 'unprimed' coordinate system, and *y'* and *z'* are the distances to the most anterior fiber in the section from the neutral axis through the section. The section properties were determined using the BoneJ plugin for ImageJ.[29] The primed coordinate system is aligned with the principal (I_{min}, I_{max}) coordinates of the bone section; the loading axes and the principal inertia property axes were generally aligned so that *ϕ* was small, and I'_z was approximately I_{min}, as has been noted previously.[30] The section modulus ($Z_{min} = I_{min}/C$) was also calculated as an outcome measure of the diaphysis. *Flexural strength* was calculated at the peak applied moment, *flexural yield strength* was calculated at the 0.2% yield offset, and *flexural modulus* was calculated as the slope of the stress-strain curve. Strain for the most anterior fiber:

$$\varepsilon = 4 \frac{c\delta}{S^2} \quad \text{[Eqn 3]}$$

where δ is the displacement of the midspan of the femur during loading and c and S are described above. It should be noted however that these estimates of cortical bone material strength do not capture the non-linear progression of failure due to the non-uniform stress field applied to the femur. Only stress on the most anterior fiber of the diaphysis is calculated without reference to the local yielding response or the progression of yielding through the bone. However, calculating fiber stress does provide a measure of the material properties of the bone without the confounding effects of changes in bone shape or size. The term flexural properties are often used to differentiate these mechanical properties from those determined using (nominally) uniform stress/strain experiments. Thus, the *bending strength* reflects the mechanical strength of the femur as an intact unit, while the *flexural strength* reflects the mechanical strength of the material (bone tissue).

Statistical Analysis

The right irradiated limb (RTx, n = 84) and left contralateral limb (Contralateral, n = 84) of the mice receiving fractionated irradiation were used in this study, as were the right limbs of sham mice (Sham, n = 72). Sham mice were not required for the -0.6 week pre-treatment time point.

Analysis of Covariance (ANCOVA) was used to assess the effects of the primary independent variable (irradiation), on the dependent variables (morphology and mechanics) with time as a covariate. Linear models were created with time as a continuous variable, the treatment (RTx vs. Sham) or (Contralateral vs. Sham) as a fixed effect, and the interaction term (RTx*time or Contralateral*time) to test differences in slope for the time vs. dependent variable response. As the goal of this study was to fully characterize the morphology and mechanics of the femur over time due to irradiation, a large number of outcome measures were used. Because ANCOVA was performed on each outcome measure, issues of multiple comparisons should be considered. To this end, we report the unmodified ANCOVA results with $p<0.05$ indicating statistical significance, but also indicate statistical significance with a very conservative Bonferroni correction of ($p < 0.002$, ~0.05/25 outcome measures). The corrected estimate is likely very conservative because many of the outcome measures are highly correlated with each other, which increases the probability of Type II error. Multiple linear regression models were used to determine if the variation in femur bending strength and post-yield displacement could be explained by the variation in geometry (section property of femur) and mineral density (TMD) for the population of sham and RTx groups.

RESULTS

Loss of metaphyseal trabecular bone (Figure 2) was grossly apparent in irradiated femurs four weeks after treatment, persisting through week 26. In the Sham group, a natural age-related progression of metaphyseal trabecular bone loss is visible during the twenty-six week period. The Contralateral group grossly appears to have fewer trabeculae compared to the Sham group, but more than the RTx group. Thickening of the metaphyseal cortical bone is evident in the RTx group following loss of trabecular bone.

Cortical Bone Morphology

At the mid-diaphysis, cortical area increased with time for all groups (see ANCOVA results, Table 1), but the rate of increase was lower for the RTx and Contralateral group compared to the Sham group (Figure 3A). Much of the reduction in cortical area can be attributed to a thinner cortex for the RTx and Contralateral groups (Figure 3B), as the endosteal area decreased with time, but was not different between groups (Figure 3C). The overall bone size (Figure 3D) was reduced for the RTx group compared to Sham, but not for the Contralateral compared to Sham. At 12 weeks, there was a reduction in cortical area (Ct.Ar = -8.3%, p = 0.006), thickness (Ct.Th = -8.1%, p = 0.002) and total area (Tt.Ar = -3.7%, p = 0.100) for the RTx versus Sham group. Normalizing to animal body weight, the reduction in cortical area (Ct.Ar/gr = -8.4%, p = 0.006) remained, indicating that this reduction was not due to change with mouse body size. At the mid-diaphysis, there is also some evidence of a systemic effect of irradiation, as the Contralateral group exhibited a reduced cortical thickness with time compared to the Sham group.

In contrast to the mid-diaphysis, there was a substantial increase in cortical area in the metaphyseal region (Table 1) for the RTx group compared to the Sham group (Figure 4A). Cortical thickness also increased more rapidly with time for the RTx versus Sham group (Figure 4B). Note that total area was not calculated for the metaphyseal cortical bone because that particular measure was very sensitive to axial position, due the rapidly changing bone shape in the metaphysis of the distal femur. At 12 weeks, there was an increase in cortical area (Ct.Ar = 11.5%, p = 0.001) and thickness (Ct.Th = 25.5%, p < 0.001) for the RTx group compared to Sham group. The metaphyseal cortical area for the Contralateral and Sham groups did not increase with time, and were not different between groups (Table 1). Thickening of the metaphyseal cortex in the RTx group was not, therefore, due to age- or body mass-related changes. Cortical thickness was nominally greater for the Sham group compared to the Contralateral group.

Trabecular Bone Morphology

There was an initial increase (week 0, 4 days after start of RTx regime) in metaphyseal trabecular bone volume for the RTx compared to Sham groups (Figure 5A). But at later time points, there was a reversal with rapid loss of trabecular bone in the RTx group compared to the Sham group (Table 1), resulting in a compartment nearly void of trabecular structure. Trabecular number and connectivity decreased with time (Figure 5B, C), but decreased at a faster rate for the RTx group. There was also an early increase in trabecular thickness for the RTx group (Figure 5D). At 12 weeks, there was a reduction in bone volume fraction (BV/TV = -69%, p < 0.001), trabecular number (Tb.N = -79%, p < 0.001) and connectivity density (Conn.D = -93%, p < 0.001) for the RTx versus Sham group. There is some evidence of systemic effects for the Contralateral group with reduced bone volume fraction, trabecular number, and connectivity compared to Sham controls (Table 1).

In the epiphyseal compartment of the distal femur, similar trends of loss of trabecular bone were found for the RTx group (Figure 6A-C). There was reduced bone volume fraction, trabecular number and connectivity density for the RTx group (Table 1), but these did not diminish to the same extent as found in the metaphyseal compartment. The remaining

trabeculae were much thicker for the RTx group at later time points (Figure 6D). At 12 weeks, there was a reduction in bone volume fraction (BV/TV = -21%, p = 0.005), trabecular number (Tb.N = -30%, p < 0.001) and connectivity density (Conn.D = -51%, p < 0.001) with an increase in trabecular thickness (Tb.Th = 12%, p = 0.001) for the RTx versus Sham group. The Contralateral group had less epiphyseal trabecular bone compared to the Sham group, with reduced BV/TV, trabecular number, and connectivity density, but this decrease was less severe than changes found with the RTx group.

Tissue Mineral Density

Tissue mineral density (TMD) of all compartments and groups increased with time (Table 1). The increase in diaphyseal TMD was greater for the Sham group with time compared to the RTx group (Figure 7A). At early time points (1–4 weeks), the trabecular TMD of the metaphysis and epiphysis for the RTx group was higher compared to the sham group (Figure 7B, C).

Femur Mechanics

The whole femur bending strength (Figure 8A) and bending stiffness (Figure 8B), measured using 3-point bend loading of the diaphysis, increased with time, but the rate of increase was greater for the Sham group compared to the RTx group (Table 1). After normalizing to mouse body weight (Figure 8C), the relative strength of the Sham group compared to RTx group remained. There was even a moderate decrease in normalized bending strength at intermediate time points (2-8 weeks) for the RTx mice suggesting that mice in this subgroup might be at greater risk of bone fracture (assuming loading demand is constant longitudinally). At twelve weeks, the RTx group had reduced bending strength (-14.1%, p = 0.005), bending stiffness (-13.3%, p = 0.0002), and normalized bending strength (-13.5%, p = 0.001) compared to the Sham group. Energy to break decreased with time (Figure 8D), but there was no significant difference between the RTx and Sham groups. Post yield displacement also decreased with time (Figure 8E), and was greater for the RTx group. There was also an apparent systemic loss of bending strength and stiffness with time for the contralateral limb (Table 1).

Diaphyseal Bone Mechanics

Flexural strength of the cortical bone increased with time, and was higher for the Sham group compared to the RTx group (Figure 9A). Flexural yield strength was not significantly different (Figure 9B) between the RTx and Sham groups, but it should be noted that the response with time was not monotonically increasing. The flexural modulus also increased with time and was higher for the Sham group (Figure 9C). At twelve weeks, the RTx group had reduced flexural strength (-5.7%, p = 0.005), flexural yield strength (-3.6%, p = 0.028) and flexural modulus (-4.9%, p = 0.0036) compared to the Sham group. There were not significant differences in the cortical bone mechanics measures for the Contralateral and Sham groups.

Contributions of Geometry, TMD, and Material Properties to Femur Strength

Using a multiple linear regression (Table 2), femur strength ($r^2 = 0.88$, $p < 0.0001$) was found to increase with diaphyseal TMD ($p < 0.0001$), and section modulus ($p < 0.0001$). However, it should be noted that RTx was associated with (reduced) section modulus ($r^2 = 0.57$), and (reduced) diaphyseal TMD ($r^2 = 0.812$) using ANCOVA in Table 1. Flexural strength of the cortical bone was also proportional to diaphyseal TMD ($r^2 = 0.55$, $p < 0.0001$).

For femurs in the later end point groups (12 to 26 weeks) there was a 15.3% decrease in femur strength for the RTx group compared to the Sham group, and it would be expected that femur strength would have contributions from bone cross section size and material strength. There was a larger contribution from bone size (section modulus decreased 12.1%) and smaller contribution from reduced material properties (flexural strength decreased 3.4%), for the RTx group compared to the Sham group. This suggests that RTx-induced reductions in diaphyseal femur strength occur predominantly through reduced bone size, and to a lesser extent through reduced material properties.

Contributions of Geometry, TMD, and Material Properties to Post-Yield Behavior

A regression model was used to determine the relationship between post-yield displacement as a measure of post-yield response with independent variables of bone size and mineralization. Post-yield displacement ($r^2 = 0.27$, $p < 0.0001$) was inversely correlated with diaphyseal TMD ($p < 0.0001$), but not section modulus ($p = 0.673$). As TMD was diminished in the RTx group compared to the Sham group, these results suggest that the post-yield properties of bone may be due in part to alterations in cortical bone mineral content.

DISCUSSION

The overall picture of post-radiotherapy bone damage in this animal model is one of diminished diaphyseal cortical bone quantity, loss of metaphyseal trabecular bone, and—to a lesser extent—loss of epiphyseal trabecular bone. Data from histological and biochemical analyses indicate roles for both altered cellular activity (osteoclasts, osteoblasts, adipocytes) and extracellular matrix modifications (alignment, crosslinking) in radiotherapy-induced bone disease (Figure 10).[6,10,13,16,17] In this model, the increase in metaphyseal cortical bone quantity may represent a compensatory response to the biomechanical effects of metaphyseal trabecular bone resorption.[31,32] Interestingly the short-term changes, occurring in this model at one week post-RTx, do not reflect that later persistent changes in bone quantity or strength.

Combined animal model data from work by our lab and others clearly demonstrates that post-radiotherapy bone damage varies according to time, dose, and volume of tissue irradiated. Work in mouse models (total body and limited field RTx) consistently demonstrates an early increase in osteoclast numbers at 1-2 weeks post-RTx, followed by long-term depletion of osteoclasts.[9,10] This results in early loss of trabecular bone, and persistence of highly crosslinked, highly aligned bone matrix due to loss of remodeling

activity.[16,17,21,33] At this point it is unknown whether loss of local osteoclasts following limited field irradiation is due to 1) the absence of osteoclast progenitor cells, or 2) an inability of osteoclast precursors to multinucleate, differentiate, or adhere. Using this mouse model, we have previously shown that mineral apposition rate is not decreased post-RTx.[10] However, other groups have shown that focal RTx results in damage to osteoblastic progenitors in a mouse model.[34] It is probable that osteoblast and marrow stromal cell responses post-RTx vary with exposure, time, cell type, and anatomic location as well. Responses of specific cell types could be addressed with a lineage tracing study.

Post-RTx changes to cortical bone mass vary by anatomic location. Data presented here describe decreased diaphyseal bone quantity late post-RTx (cortical thickness, area, and density). Metaphyseal cortical bone, however, increased in thickness, possibly as a mechanical adaptation to compensate for loss of adjacent metaphyseal trabecular bone. Indeed, a previous histological study demonstrated that post-RTx bone mineral apposition continued normally at the endocortical and periosteal surfaces of the metaphysis.[10]

Results from our model contrast somewhat with those of Wright et al., who found decreased femoral trabecular BV/TV, Tb.N, and increased Tb.Sp in irradiated femora (compared to sham controls) seven days after exposure to a single 2 Gy X-ray treatment.[13] The different results could be explained both by the radiation dose (4x5 Gy vs. 1x2 Gy), and the timing between irradiation and tissue harvest. We have previously found that the time course of osteoclast activity and trabecular resorption varies depending on when the last dose of radiation is delivered.[10]

Following irradiation, loss of functional bone strength (bending strength) appears to result from both decreased bone size (relative to age-matched sham controls), decreased diaphyseal TMD, and diminished material properties. The role of TMD and material properties is highlighted by the fact that normalizing bending strength to body mass did not alter this outcome (as was expected given that the body weights of the irradiated and sham mice were not different at later time points). We have previously quantified post-RTx changes to bone biochemistry in this mouse model that may contribute to loss of material strength (Figure 10). Most notably, post-RTx bone matrix is characterized by an increased trivalent:divalent collagen crosslink ratio, suggesting that collagen is overly mature.[16,17] Collagen and mineral alignment are also increased post-RTx; this loss of tissue heterogeneity may contribute to bone fragility by decreasing fracture toughness. Finally, irradiated bone contains more advanced glycation end products, which can also contribute to tissue embrittlement.[18] The abscopal effects of radiation on bone biochemistry are not well characterized, and worthy of further investigation. Future work to determine the direct contributions of radiation-diminished material properties to bone fragility is needed, including assessment of fracture toughness. The abscopal effects of limited field irradiation on femur strength in other loading modalities, such as axial compression, are also not currently known.

The systemic or abscopal effects of limited field irradiation on the contralateral non-irradiated femur in this model tended towards an intermediate response (between RTx and sham). Metaphyseal and epiphyseal BV/TV, Tb.N, and Conn.D, as well as cortical thickness,

TMD, and bending strength were all significantly decreased in contralateral femurs relative to sham group femurs, but to a lesser magnitude than the irradiated femurs. The extent of systemic damage following limited field radiotherapy motivates further study to identify mechanisms of action and potential therapeutics, and highlights the need for longitudinal clinical studies of local and systemic bone density and fracture risk assessment in post-radiotherapy cancer survivors.

The results of clinical studies have identified several risk factors for post-RTx fragility fractures, including the patient's pre-treatment BMD, menopausal status, and volumetric radiation dose to bone. Decreased pre-treatment bone density (determined by computed tomography, or CT) has been associated with increased risk of post-irradiation pelvic insufficiency fractures in patients with uterine cervical cancer.[35] Clinical studies report varied effects of radiotherapy on BMD, ranging from significantly decreased vertebral BMD in survivors of abdominal cancers[36] and patients undergoing pelvic radiotherapy for cervical cancer,[37] to no change in extremity BMD for survivors of soft tissue sarcoma.[7]

Few studies have examined BMD at non-irradiated sites in patients post-radiotherapy. Examining vertebral BMD in post-menopausal cervical cancer survivors one to seven years after radiotherapy, Chen et al. found no significant decrease in either irradiated or non-irradiated BMD as determined by dual-energy X-ray absorptiometry (DXA).[8] A separate longitudinal study of cervical cancer patients undergoing pelvic radiotherapy found decreased BMD in non-irradiated vertebrae only in pre-menopausal patients.[37] In survivors of extremity soft tissue sarcomas, Dhakal et al. found regional BMD for bone within the irradiated field did not consistently decrease post-radiotherapy when compared to ipsilateral and contralateral non-irradiated tissue sites.[7] Because all BMD measurements were made after radiotherapy, and control tissue sites were identified from within the irradiated individual, the study did not account for the possibility of abscopal effects. While Dhakal et al. found slightly decreased BMD in regions contralateral to the irradiated bone; this was ascribed to disuse-type osteopenia.[7]

Our data suggest additional longitudinal studies may be necessary to definitively determine the association between radiotherapy and local vs. systemic alterations (or lack thereof) in bone mineral density. In a study following eighteen women who received pelvic radiotherapy for cervical carcinoma, Blomlie et al. found that although 89% of the patients experienced fractures, none were located outside the irradiation field.[38] Another study of 6,428 older women (age 65 yrs) found no association between pelvic radiotherapy and arm or spine fractures, suggesting that fracture risk may not increase at sites distant to the irradiated field.[39] Elliott et al. reviewed a cohort of 45,662 prostate cancer survivors, and found that external beam radiation therapy did not increase the risk for bone fracture outside the field of radiation (distal forearm).[40] Radiotherapy was, however, associated with a 76% increased risk of hip (irradiated bone) fracture in these patients. Clinical data is, at this point, insufficient to determine if fracture risk is definitively increased for patients at non-irradiated sites.

The animal model-derived data presented here, and that from other labs,[13,20] indicate that limited field irradiation can result in significant systemic bone damage. These findings

suggest that the ideal control sample would be a pre-radiotherapy CT or DXA measurement of bone volume and density. Studies that rely on non-irradiated tissue from within the patient as a control for radiotherapy-induced bone damage should be interpreted with caution, as this design does not account for abscopal effects. Furthermore, data presented here indicate that responses of bone to radiotherapy, via either direct or abscopal damage, vary by anatomic compartment.

The abscopal effects of limited field irradiation on bone clearly indicate systemic damage, possibly mediated through elevated systemic oxidative stress or other soluble inflammatory factors (e.g. cytokines, peroxidized lipids, glycation end products, reactive oxygen species). [41-43] In addition to morphologic changes, our study demonstrated significant loss of functional (bending) strength in the contralateral mouse femurs. Additional clinical investigation is needed to determine the extent to which strength is diminished in bone distant to the radiation field, and if this loss of strength impacts fracture risk.

There are several limitations to this small animal model, including the small volume of trabecular bone present in mice, low forces applied during daily ambulation/skeletal loading, and short life span, which constrain our ability to translate these findings directly to human clinical care. Nevertheless, this work recapitulates the clinical observation of increased fracture risk/decreased bone strength within the radiation field. Our animal model data furthermore establishes that there are abscopal or systemic effects of limited field irradiation, and that time post-irradiation is a key variable in determining the severity of response. These findings suggest that pre-irradiation measurements may be the best control for clinical studies of radiotherapy effects on bone density or fracture risk, given the potentially significant effects of radiotherapy on distant bone tissues within the patient.

Acknowledgments

References

1. Dickie CI, Parent AL, Griffin AM, Fung S, Chung PW, Catton CN, et al. Bone fractures following external beam radiotherapy and limb-preservation surgery for lower extremity soft tissue sarcoma: relationship to irradiated bone length, volume, tumor location and dose. Int J Radiat Oncol Biol Phys. Nov 15; 2009 75(4):1119–24. Epub 2009/04/14. [PubMed: 19362782]

2. Cannon CP, Ballo MT, Zagars GK, Mirza AN, Lin PP, Lewis VO, et al. Complications of combined modality treatment of primary lower extremity soft-tissue sarcomas. Cancer. Nov 15; 2006 107(10): 2455–61. [PubMed: 17036354]

3. Oh D, Huh SJ, Nam H, Park W, Han Y, Lim do H, et al. Pelvic insufficiency fracture after pelvic radiotherapy for cervical cancer: analysis of risk factors. Int J Radiat Oncol Biol Phys. Mar 15; 2008 70(4):1183–8. Epub 2007/10/09. [PubMed: 17919836]

4. Paulino AC. Late effects of radiotherapy for pediatric extremity sarcomas. Int J Radiat Oncol Biol Phys. Sep 1; 2004 60(1):265–74. [PubMed: 15337565]

5. Bandstra ER, Pecaut MJ, Anderson ER, Willey JS, De Carlo F, Stock SR, et al. Long-term dose response of trabecular bone in mice to proton radiation. Radiat Res. Jun; 2008 169(6):607–14. Epub 2008/05/23. [PubMed: 18494551]

6. Green DE, Adler BJ, Chan ME, Rubin CT. Devastation of adult stem cell pools by irradiation precedes collapse of trabecular bone quality and quantity. J Bone Miner Res. Apr; 2012 27(4):749–59. Epub 2011/12/23. [PubMed: 22190044]

7. Dhakal S, Chen J, McCance S, Rosier R, O'Keefe R, Constine LS. Bone density changes after radiation for extremity sarcomas: exploring the etiology of pathologic fractures. Int J Radiat Oncol Biol Phys. Jul 15; 2011 80(4):1158–63. Epub 2010/10/05. [PubMed: 20888134]

8. Chen HH, Lee BF, Guo HR, Su WR, Chiu NT. Changes in bone mineral density of lumbar spine after pelvic radiotherapy. Radiother Oncol. Feb; 2002 62(2):239–42. [PubMed: 11937252]

9. Willey JS, Lloyd SA, Robbins ME, Bourland JD, Smith-Sielicki H, Bowman LC, et al. Early increase in osteoclast number in mice after whole-body irradiation with 2 Gy X rays. Radiat Res. Sep; 2008 170(3):388–92. Epub 2008/09/04. [PubMed: 18763868]

10. Oest ME, Franken V, Kuchera T, Strauss J, Damron TA. Long-term loss of osteoclasts and unopposed cortical mineral apposition following limited field irradiation. J Orthop Res. Mar; 2015 33(3):334–42. [PubMed: 25408493]

11. Green DE, Adler BJ, Chan ME, Lennon JJ, Acerbo AS, Miller LM, et al. Altered composition of bone as triggered by irradiation facilitates the rapid erosion of the matrix by both cellular and physicochemical processes. PLoS One. 2013; 8(5):e64952. Epub 2013/06/07. [PubMed: 23741433]

12. Nyaruba MM, Yamamoto I, Kimura H, Morita R. Bone fragility induced by X-ray irradiation in relation to cortical bone-mineral content. Acta Radiol. Jan; 1998 39(1):43–6. Epub 1998/03/14. [PubMed: 9498868]

13. Wright LE, Buijs JT, Kim HS, Coats LE, Scheidler AM, John SK, et al. Single-Limb Irradiation Induces Local and Systemic Bone Loss in a Murine Model. J Bone Miner Res. Jul; 2015 30(7): 1268–79. [PubMed: 25588731]

14. Chandra A, Lan S, Zhu J, Lin T, Zhang X, Siclari VA, et al. PTH prevents the adverse effects of focal radiation on bone architecture in young rats. Bone. Aug; 2013 55(2):449–57. Epub 2013/03/08. [PubMed: 23466454]

15. Hopewell JW. Radiation-therapy effects on bone density. Med Pediatr Oncol. Sep; 2003 41(3):208–11. Epub 2003/07/18. [PubMed: 12868120]

16. Gong B, Oest ME, Mann KA, Damron TA, Morris MD. Raman spectroscopy demonstrates prolonged alteration of bone chemical composition following extremity localized irradiation. Bone. Nov; 2013 57(1):252–8. Epub 2013/08/28. [PubMed: 23978492]

17. Oest ME, Gong B, Esmonde-White K, Mann KA, Zimmerman ND, Damron TA, et al. Parathyroid hormone attenuates radiation-induced increases in collagen crosslink ratio at periosteal surfaces of mouse tibia. Bone. May.2016 86:91–7. [PubMed: 26960578]

18. Oest ME, Damron TA. Focal therapeutic irradiation induces an early transient increase in bone glycation. Radiat Res. Apr; 2014 181(4):439–43. Epub 2014/04/08. [PubMed: 24701964]

19. Wernle JD, Damron TA, Allen MJ, Mann KA. Local irradiation alters bone morphology and increases bone fragility in a mouse model. J Biomech. Oct 19; 2010 43(14):2738–46. Epub 2010/07/27. [PubMed: 20655052]

20. Zou Q, Hong W, Zhou Y, Ding Q, Wang J, Jin W, et al. Bone marrow stem cell dysfunction in radiation-induced abscopal bone loss. Journal of orthopaedic surgery and research. 2016; 11:3. [PubMed: 26739584]

21. Willey JS, Livingston EW, Robbins ME, Bourland JD, Tirado-Lee L, Smith-Sielicki H, et al. Risedronate prevents early radiation-induced osteoporosis in mice at multiple skeletal locations. Bone. Jan; 2010 46(1):101–11. Epub 2009/09/15. [PubMed: 19747571]

22. Keenawinna L, Oest ME, Mann KA, Spadaro J, Damron TA. Zoledronic acid prevents loss of trabecular bone after focal irradiation in mice. Radiat Res. Jul; 2013 180(1):89–99. Epub 2013/06/19. [PubMed: 23772924]

23. Overgaard M. Spontaneous radiation-induced rib fractures in breast cancer patients treated with postmastectomy irradiation. A clinical radiobiological analysis of the influence of fraction size and dose-response relationships on late bone damage. Acta Oncol. 1988; 27(2):117–22. Epub 1988/01/01. [PubMed: 3390342]

24. Fowler JF. Development of radiobiology for oncology-a personal view. Phys Med Biol. Jul 7; 2006 51(13):R263–86. Epub 2006/06/23. [PubMed: 16790907]

25. Rordorf T, Hassan AA, Azim H, Alexandru E, Er O, Gokmen E. Bone health in breast cancer patients: A comprehensive statement by CECOG/SAKK Intergroup. Breast. Jun 27.2014 Epub 2014/07/06.

26. Patel S, DeLaney TF. Advanced-technology radiation therapy for bone sarcomas. Cancer Control. Jan; 2008 15(1):21–37. Epub 2007/12/21. [PubMed: 18094658]

27. Bouxsein ML, Boyd SK, Christiansen BA, Guldberg RE, Jepsen KJ, Muller R. Guidelines for assessment of bone microstructure in rodents using micro-computed tomography. J Bone Miner Res. Jul; 2010 25(7):1468–86. [PubMed: 20533309]

28. Boresi, AP., Schmidt, RJ., Sidebottom, OM. Advanced mechanics of materials. 5. New York: John Wiley and Sons, Inc; 1993.

29. Doube M, Klosowski MM, Arganda-Carreras I, Cordelieres FP, Dougherty RP, Jackson JS, et al. BoneJ: Free and extensible bone image analysis in ImageJ. Bone. Dec; 2010 47(6):1076–9. Epub 2010/09/08. [PubMed: 20817052]

30. Brodt MD, Ellis CB, Silva MJ. Growing C57Bl/6 mice increase whole bone mechanical properties by increasing geometric and material properties. J Bone Miner Res. Dec; 1999 14(12):2159–66. [PubMed: 10620076]

31. Sugiyama T, Price JS, Lanyon LE. Functional adaptation to mechanical loading in both cortical and cancellous bone is controlled locally and is confined to the loaded bones. Bone. Feb; 2010 46(2): 314–21. [PubMed: 19733269]

32. Warden SJ, Hurst JA, Sanders MS, Turner CH, Burr DB, Li J. Bone adaptation to a mechanical loading program significantly increases skeletal fatigue resistance. J Bone Miner Res. May; 2005 20(5):809–16. [PubMed: 15824854]

33. Oest ME, Mann KA, Zimmerman ND, Damron TA. Parathyroid Hormone (1-34) Transiently Protects Against Radiation-Induced Bone Fragility. Calcif Tissue Int. Jun; 2016 98(6):619–30. [PubMed: 26847434]

34. Chandra A, Lin T, Zhu J, Wei T, Huo Y, Jia H, et al. PTH1-34 Blocks Radiation-Induced Osteoblast Apoptosis by Enhancing DNA Repair through Canonical Wnt Pathway. J Biol Chem. Oct 21.2014

35. Uezono H, Tsujino K, Moriki K, Nagano F, Ota Y, Sasaki R, et al. Pelvic insufficiency fracture after definitive radiotherapy for uterine cervical cancer: retrospective analysis of risk factors. J Radiat Res. Nov 1; 2013 54(6):1102–9. Epub 2013/05/21. [PubMed: 23685668]

36. Wei RL, Jung BC, Manzano W, Sehgal V, Klempner SJ, Lee SP, et al. Bone mineral density loss in thoracic and lumbar vertebrae following radiation for abdominal cancers. Radiother Oncol. Mar; 2016 118(3):430–6. [PubMed: 26993414]

37. Okonogi N, Saitoh J, Suzuki Y, Noda SE, Ohno T, Oike T, et al. Changes in bone mineral density in uterine cervical cancer patients after radiation therapy. Int J Radiat Oncol Biol Phys. Dec 1; 2013 87(5):968–74. [PubMed: 24139516]

38. Blomlie V, Rofstad EK, Talle K, Sundfor K, Winderen M, Lien HH. Incidence of radiation-induced insufficiency fractures of the female pelvis: evaluation with MR imaging. AJR Am J Roentgenol. Nov; 1996 167(5):1205–10. [PubMed: 8911181]

39. Baxter NN, Habermann EB, Tepper JE, Durham SB, Virnig BA. Risk of pelvic fractures in older women following pelvic irradiation. JAMA. Nov 23; 2005 294(20):2587–93. Epub 2005/11/24. [PubMed: 16304072]

40. Elliott SP, Jarosek SL, Alanee SR, Konety BR, Dusenbery KE, Virnig BA. Three-dimensional external beam radiotherapy for prostate cancer increases the risk of hip fracture. Cancer. Oct 1; 2011 117(19):4557–65. [PubMed: 21412999]

41. Baskar R. Emerging role of radiation induced bystander effects: Cell communications and carcinogenesis. Genome integrity. Sep 12.2010 1(1):13. [PubMed: 20831828]

42. Najafi M, Fardid R, Takhshid MA, Mosleh-Shirazi MA, Rezaeyan AH, Salajegheh A. Radiation-Induced Oxidative Stress at Out-of-Field Lung Tissues after Pelvis Irradiation in Rats. Cell J Fall. 2016; 18(3):340–5.
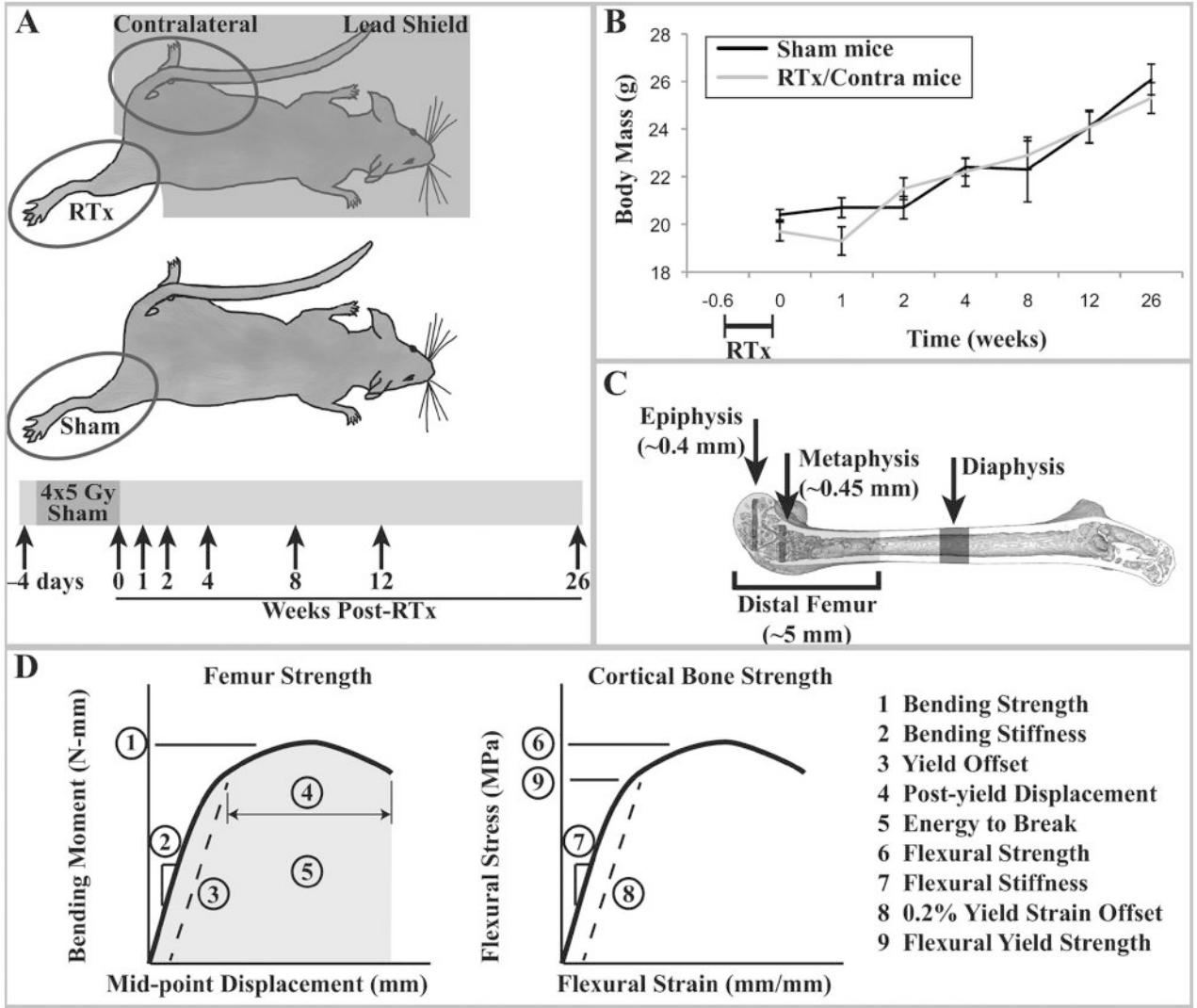
43. Rastogi S, Coates PJ, Lorimore SA, Wright EG. Bystander-type effects mediated by long-lived inflammatory signaling in irradiated bone marrow. Radiat Res. Mar; 2012 177(3):244–50. [PubMed: 22149991]
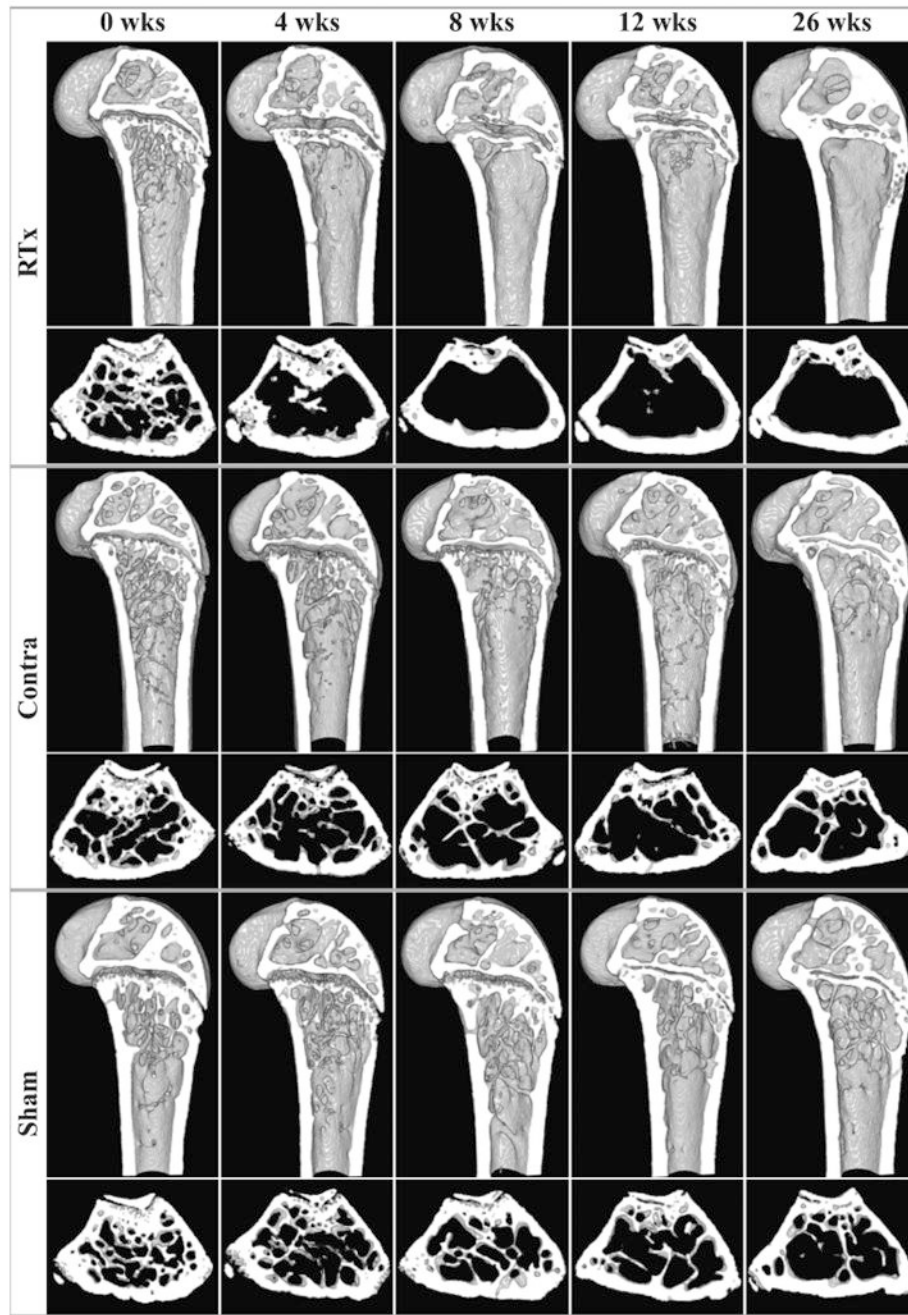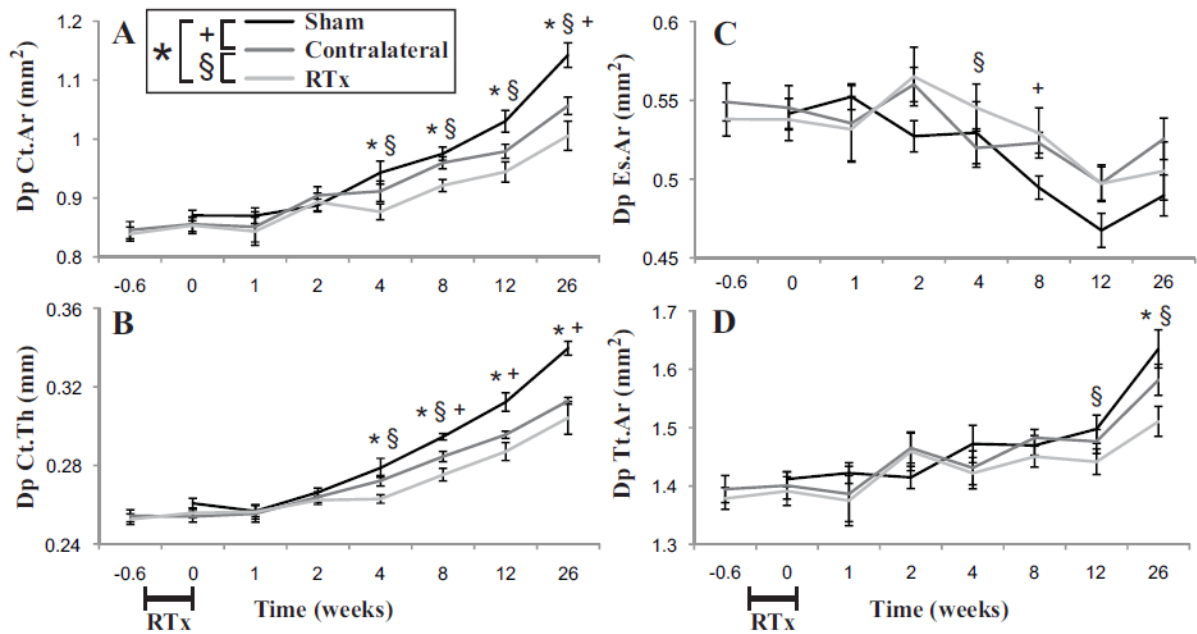
Figure 1.
A) Experimental design: female BALB/cJ mice aged 12 weeks were exposed to four consecutive daily unilateral hindlimb irradiation exposures of 5 Gy each. The contralateral hindlimb and body were shielded with lead. These animals yielded the RTx and Contra samples. A separate group of age-matched animals were anesthetized but not irradiated, yielding the Sham samples. At end points of 4 days prior to treatment and 0, 1, 2, 4, 8, 12, and 26 weeks after treatment, animals were euthanized and femurs collected. B) Average mouse body mass for each treatment group (arithmetic mean ± standard error) over the course of the study. There were no significant differences in body mass at any time point between the sham and irradiated mice (contralateral femurs are derived from the non-irradiated limb of RTx group mice). C) Schematic of the μCT volumes of interest. D) Graphical description of the femur strength and cortical bone strength outcome measures.
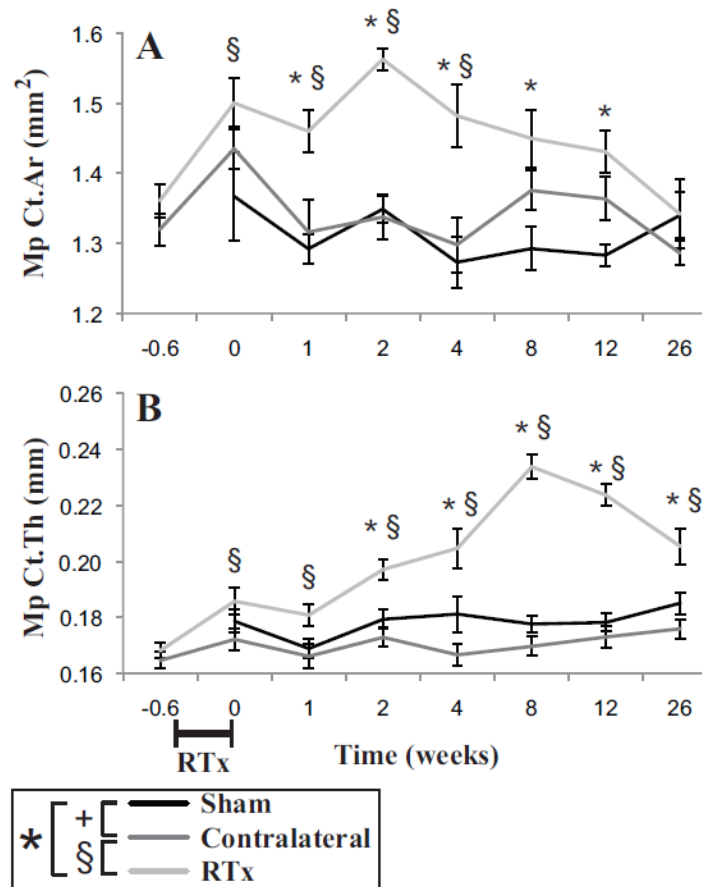
Figure 2.
Representative µCT-derived cross-sections of bones at 0, 4, 8, 12, and 26 weeks after treatment for each group. For each treatment group, the upper row presents a sagittal section of the distal femur, and the lower row presents a transverse metaphyseal cross-section.
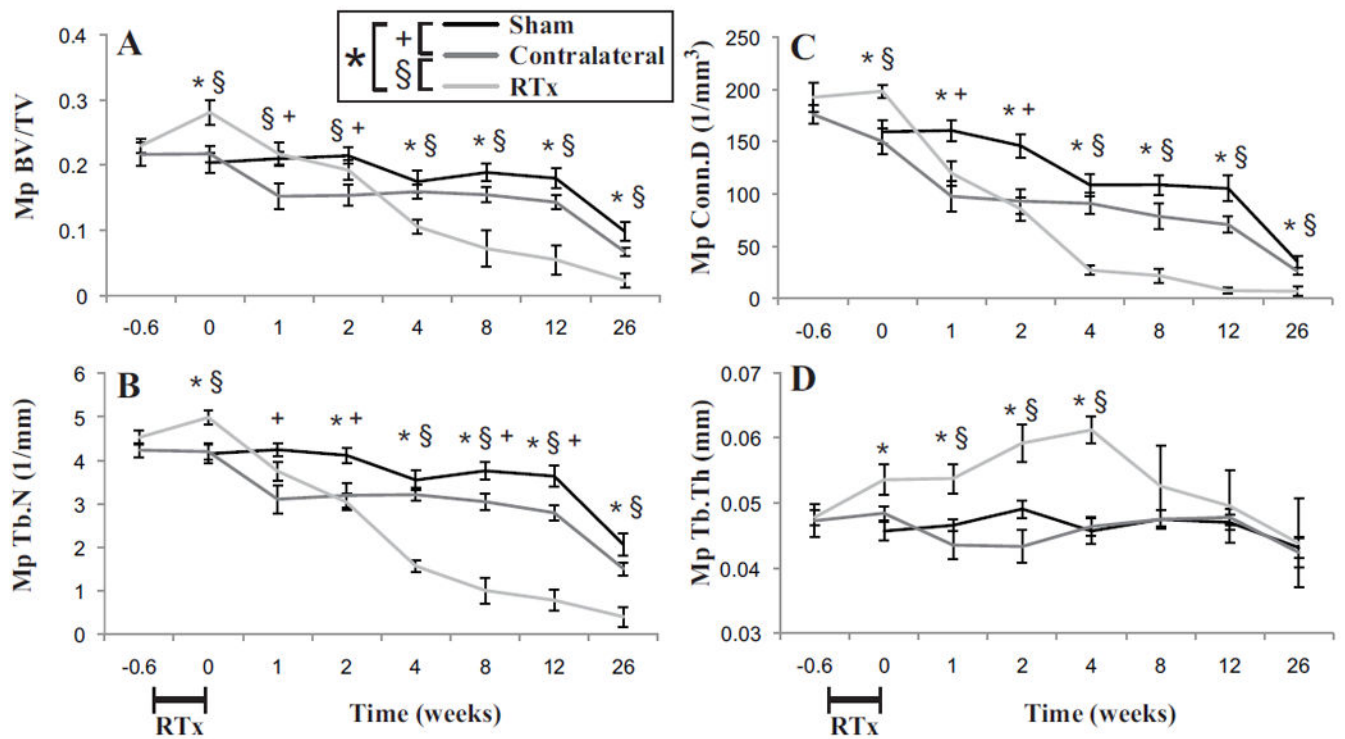
Figure 3.
Mid-diaphyseal (cortical) bone geometric parameters of femora as a function following 4x5 Gy hindlimb irradiation for Sham, Contralateral, and RTx groups. A) Cortical area (Ct.Ar); B) mean cortical thickness (Ct.Th); C) endosteal area (Es.Ar), and D) total cross sectional area (Tt.Ar) results are shown with arithmetic mean ± standard error bars. Statistically significant differences between groups are denoted for p < 0.05.
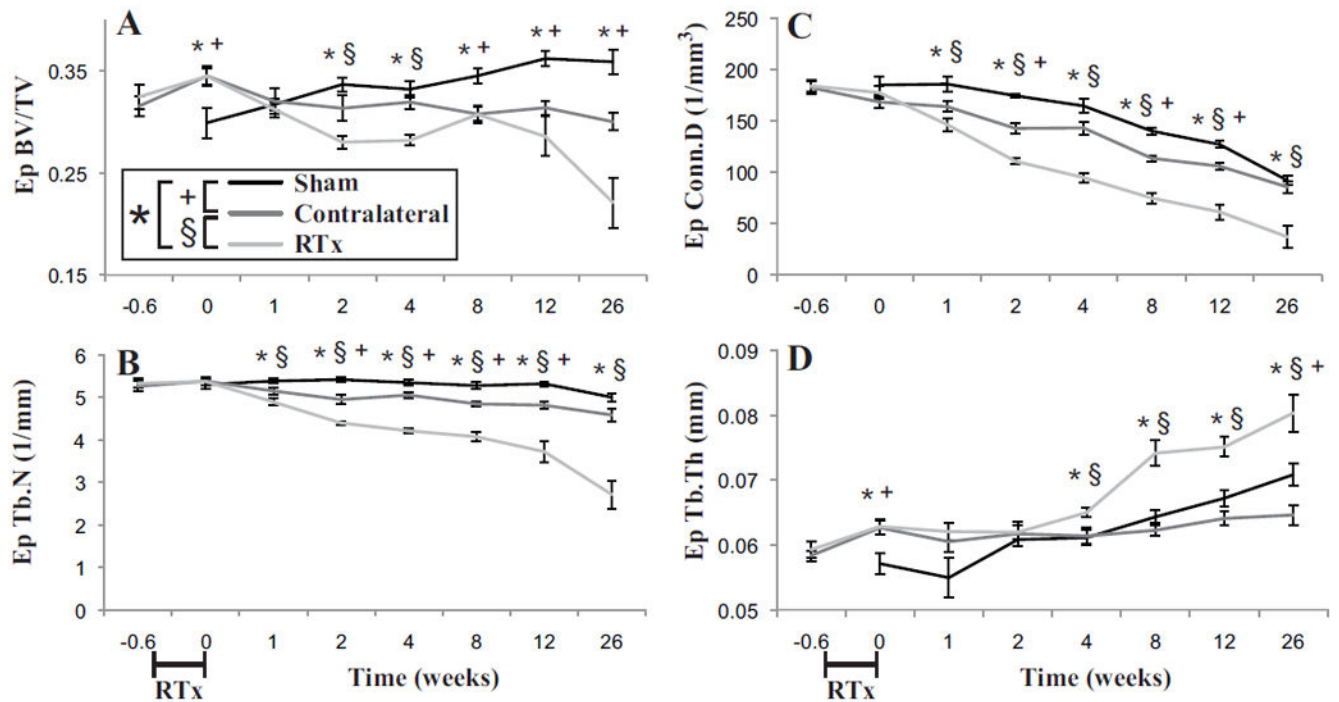
Figure 4.
Metaphyseal cortical bone of the distal femur as a function of time following 4x5 Gy hindlimb irradiation for Sham, Contralateral, and RTx groups. A) Cortical area (Ct.Ar) and B) mean cortical thickness (Ct.Th) results are shown with arithmetic mean ± standard error bars. Statistically significant differences between groups are denoted for $p < 0.05$.

Figure 5.
Metaphyseal trabecular bone of the femur as a function of time following 4x5 Gy hindlimb irradiation for Sham, Contralateral, and RTx groups. A) Bone volume fraction (BV/TV); B) trabecular number (Tb.N); C) connectivity density (Conn.D); and D) trabecular thickness (Tb.Th) results are presented as arithmetic mean ± standard error bars. Statistically significant differences between groups are denoted for $p < 0.05$.
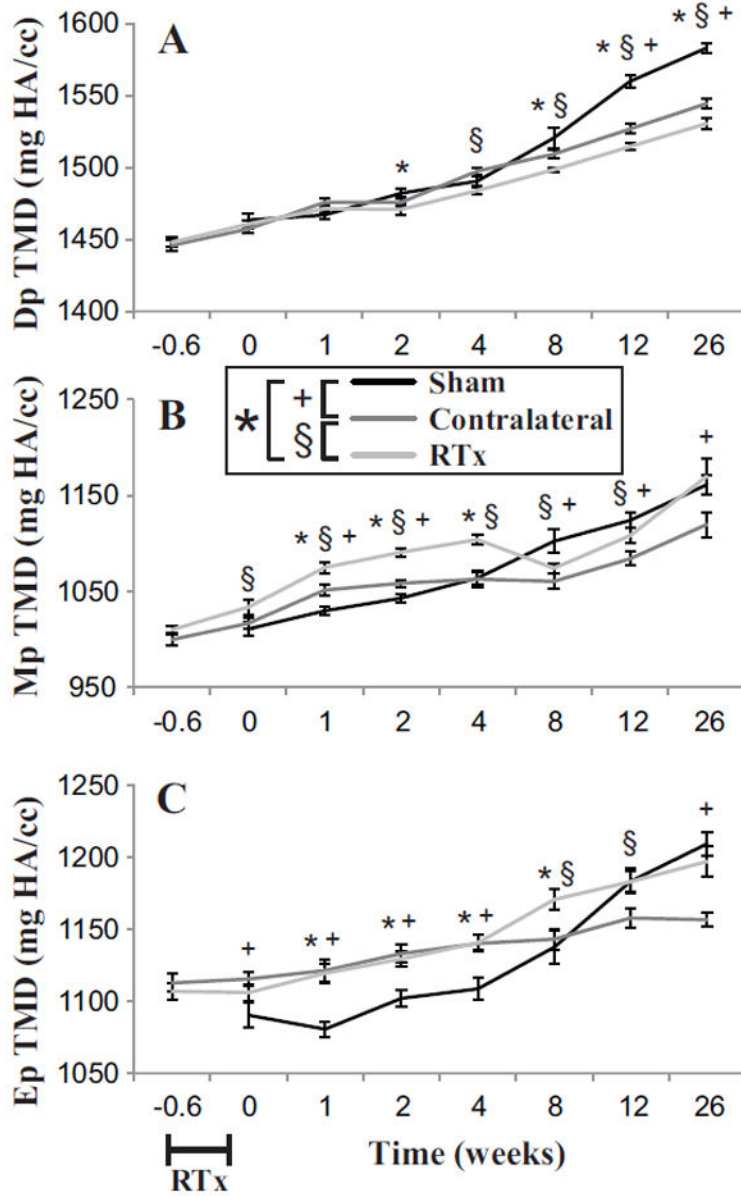
Figure 6.
Epiphyseal trabecular bone of the femur as a function of time following 4x5 Gy hindlimb irradiation for Sham, Contralateral, and RTx groups. A) Bone volume fraction (BV/TV); B) trabecular number (Tb.N); C) connectivity density (Conn.D); and D) trabecular thickness (Tb.Th) results are presented as arithmetic mean ± standard error bars. Statistically significant differences between groups are denoted for $p < 0.05$.

Figure 7.
Tissue mineral density (TMD) of the femur as a function of time following 4x5 Gy hindlimb irradiation for Sham, Contralateral, and RTx groups. Volumes of interest included A) Diaphyseal cortical (Dp TMD); B) metaphyseal trabecular (Mp TMD); and C) epiphyseal trabecular (Ep TMD). Results are presented as arithmetic mean ± standard error bars. Statistically significant differences between groups are denoted for $p < 0.05$.
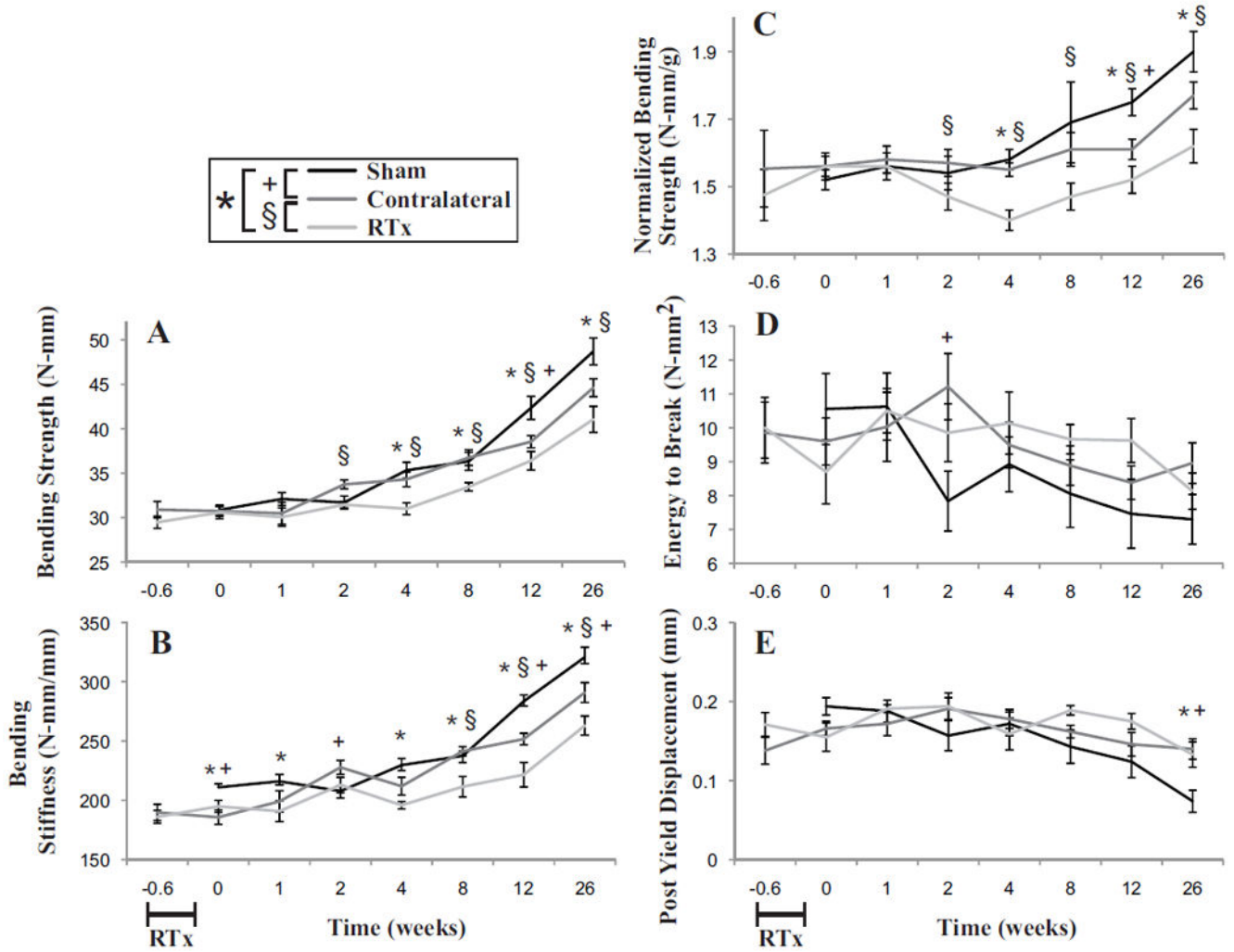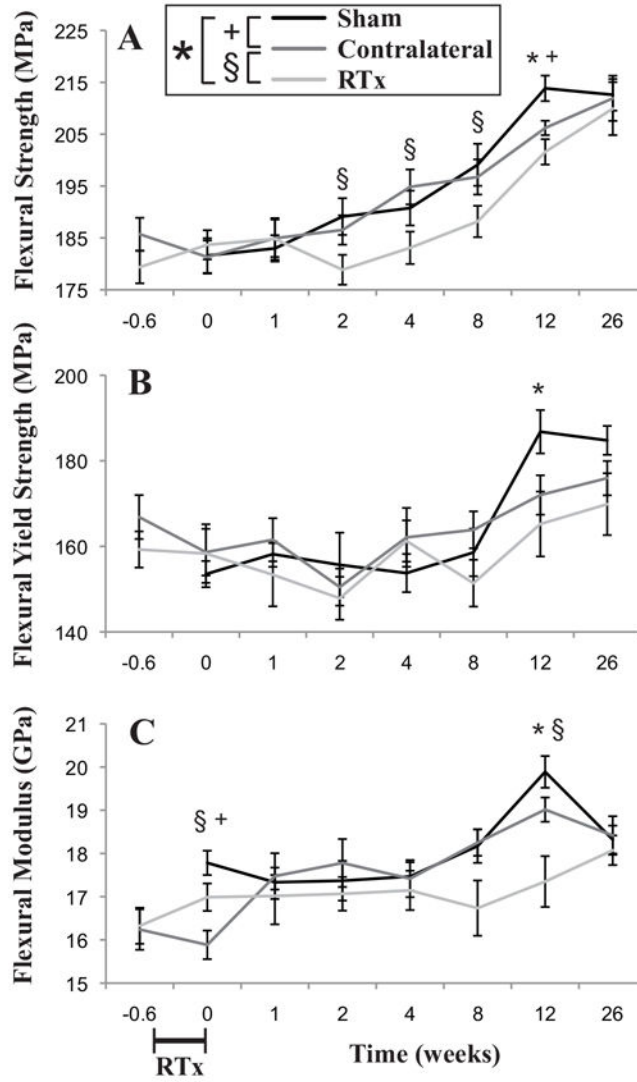
Figure 8.
Mechanical strength of the femurs in bending as a function of time following 4x5 Gy hindlimb irradiation for Sham, Contralateral, and RTx groups. A) Bending strength of the femur B) bending stiffness of the femur; C) bending strength normalized to individual mouse body weight; D) energy to break; and E) post-yield displacement. Data presented as arithmetic mean ± standard error, with significance between groups denoted at p < 0.05.

Figure 9.
Mechanical properties of the mid-diaphyseal cortical bone in bending as a function of time following 4x5 Gy hindlimb irradiation for Sham, Contralateral, and RTx groups. A) Flexural strength and B) flexural yield strength of the bone material; and C) flexural modulus of the cortical bone. Data presented as arithmetic mean ± standard error, with significance between groups denoted at p < 0.05.
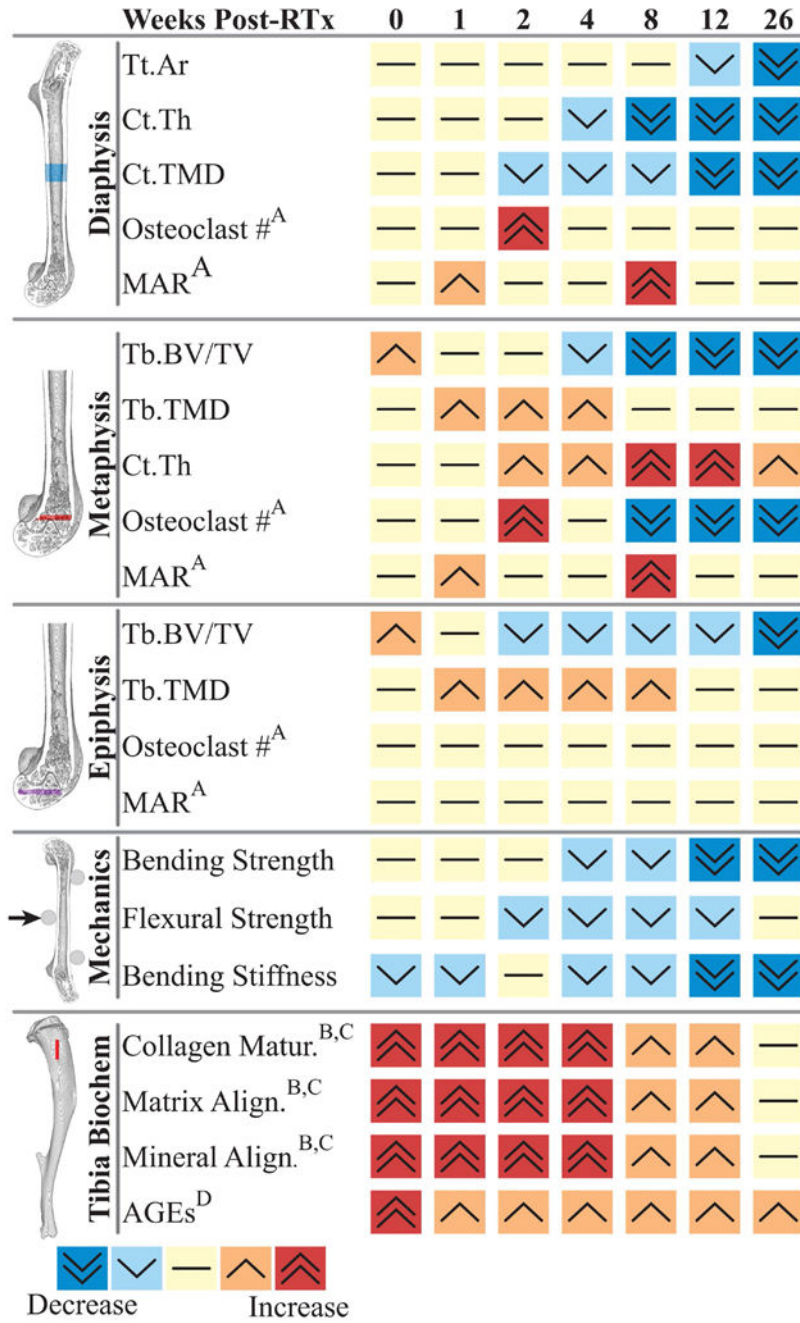
Figure 10.
Summary of post-irradiation changes in bone morphology, density, mechanics, and biochemistry as a function of time after treatment in this murine model of limited field radiotherapy. Biochemical and histomorphologic data derived from: A) Oest et al. *J Orthop Res* 2015 33(3):334-42 (ref #10); B) Gong et al. *Bone* 2013 57(1):252-8 (ref #16), C) Oest et al. *Bone* 2016 86:91-7 (ref #17), D) Oest and Damron *Radiat Res* 2014 181(4):439-43 (ref #18). **Abbreviations:** Tt.Ar: total area, Ct.Th: cortical thickness, Ct.TMD: cortical tissue mineral density, MAR: mineral apposition rate, Tb. BV/TV: trabecular bone volume

fraction, Tb.TMD: trabecular tissue mineral density, AGEs: advanced glycation end products. All studies reflected in this figure were conduced on BALB/c mice, used in several studies over many years. Mice from the study detailed in this manuscript were not the same as the mice from which osteoclast, MAR, and biochemical data were obtained.

Table 1

Analysis of Covariance (ANCOVA) results for geometric, tissue density, and mechanics outcome variables as a function of time from radiation treatment, treatment (sham vs. RTx or sham vs. contralateral), and the interaction term (time*treatment). The corresponding graphical Figures for these analyses are shown in Figures 3–9. P-values for the ANCOVA models are shown along with overall model fit (r^2)

	Region of Interest	ANCOVA: Sham vs. RTx				ANCOVA: Sham vs. Contralateral			
	Diaphyseal Cortical	*Time*	*RTx*	*Time*RTx*	r^2	*Time*	*Contra*	*Time*Contra*	r^2
Figure 3	Ct.Ar	0.0001	0.0001	0.0001	0.686	0.0001	0.0002	0.0031	0.722
	Ct.Th	0.0001	0.0001	0.0001	0.757	0.0001	0.0001	0.0001	0.831
	Es.Ar	0.0001	0.0699	0.4474	0.149	0.0001	0.0297	0.1058	0.143
	Tt.Ar	0.0001	0.0015	0.0087	0.367	0.0001	0.2143	0.2841	0.407
	Zmin	0.0001	0.0001	0.0001	0.569	0.0001	0.0118	0.334	0.570
	Metaphyseal Cortical	*Time*	*RTx*	*Time*RTx*	r^2	*Time*	*Contra*	*Time*Contra*	r^2
Figure 4	Ct.Ar	0.0417	0.0001	0.0216	0.274	0.352	0.137	0.2251	0.031
	Ct.Th	0.0001	0.0001	0.0262	0.328	0.0043	0.0001	0.8825	0.143
	Metaphyseal Trabecular	*Time*	*RTx*	*Time*RTx*	r^2	*Time*	*Contra*	*Time*Contra*	r^2
Figure 5	BV/TV	0.0001	0.0001	0.0002	0.521	0.0001	0.0002	0.5507	0.453
	Tb.N	0.0001	0.0001	0.0001	0.615	0.0001	0.0001	0.5537	0.558
	Conn.D	0.0001	0.0001	0.954	0.534	0.0001	0.0001	0.673	0.542
	Tb.Th	0.0092	0.0019	0.19	0.117	0.0161	0.4769	0.806	0.039
	Epiphyseal Trabecular	*Time*	*RTx*	*Time*RTx*	r^2	*Time*	*Contra*	*Time*Contra*	r^2
Figure 6	BV/TV	0.0203	0.0001	0.0001	0.4	0.1399	0.0001	0.0001	0.215
	Tb.N	0.0001	0.0001	0.0001	0.717	0.0001	0.0001	0.0359	0.394
	Conn.D	0.0001	0.0001	0.0104	0.715	0.0001	0.0001	0.427	0.722
	Tb.Th	0.0001	0.0001	0.0206	0.569	0.0001	0.8008	0.0001	0.337
	Tissue Mineral Densities	*Time*	*RTx*	*Time*RTx*	r^2	*Time*	*Contra*	*Time*Contra*	r^2
Figure 7	Dp	0.0001	0.0001	0.0001	0.833	0.0001	0.0001	0.0001	0.812
	Mp	0.0001	0.0218	0.1791	0.634	0.0001	0.0009	0.001	0.658
	Ep	0.0001	0.0001	0.004	0.659	0.0001	0.1119	0.0001	0.616
Figure 8	**Femur Mechanics**	*Time*	*RTx*	*Time*RTx*	r^2	*Time*	*Contra*	*Time*Contra*	r^2

Region of Interest	ANCOVA: Sham vs. RTx				ANCOVA: Sham vs. Contralateral			
Bending Strength	0.0001	0.0001	0.0001	0.74	0.0001	0.0188	0.0036	0.757
Bending Stiffness	0.0001	0.0001	0.0001	0.728	0.0001	0.0001	0.0619	0.744
Post-Yield Displacement	0.0001	0.0154	0.0018	0.26	0.0001	0.191	0.0003	0.249
Energy to Break	0.001	0.0503	0.371	0.095	0.0017	0.0582	0.3014	0.08
Bend Strength/BW	0.0001	0.0001	0.0002	0.387	0.0001	0.4264	0.0111	0.373
Cortical Bone Mechanics	*Time*	*RTx*	*Time*RTx*	*r²*	*Time*	*Contra*	*Time*Contra*	*r²*
Flexural Strength	0.0001	0.0042	0.794	0.487	0.0001	0.6736	0.6057	0.472
Flexural Yield Strength	0.0001	0.0812	0.0316	0.196	0.0001	0.879	0.027	0.23
Flexural Modulus	0.0003	0.0002	0.985	0.165	0.0001	0.1091	0.2812	0.161

Figure 9

Abbreviations: Ct.Ar: cortical area, Ct.Th: cortical thickness, Es.Ar: endosteal area, Tt.Ar: total area, Zmin: section modulus, BV/TV: bone volume fraction, Tb.N: trabecular number, Conn.D: connectivity density, Tb.Th: trabecular thickness, Dp: diaphyseal, Mp: metaphyseal, Ep: epiphyseal, BW: body weight.

Table 2

Multiple regression models relating mechanical outcome measures (bending strength and post-yield displacement) with geometry (section modulus) and tissue density (TMD). Estimate values and significance level of each are listed, along with an overall model fit.

	Summary of Fit (n = 153)	Intercept	Section Modulus (Zmin, mm^3)	Tissue Mineral Density (TMD, mg HA/cc)
Femur Bending Strength (N-mm)	$r^2 = 0.88$ (p < 0.0001)	-101.9 (p < 0.0001)	159.3 (p < 0.0001)	0.0721 (p < 0.0001)
Post-Yield Displacement (mm)	$r^2 = 0.20$ (p < 0.0001)	1.08 (p < 0.0001)	-0.146 (p = 0.579)	-0.000598 (p < 0.0001)